CHAPTER 4
EXPERIMENTAL SET-UP

The entire experimental programme has been listed in *Plan of Work (Chapter 1)*. This chapter outlines the details of the raw materials, apparatus, and experimental procedures followed in the present investigation. A comprehensive experimental programme was designed for characterization of raw materials, preparation and testing of iron ore-coal composite briquettes / pellets and fundamental investigation on reduction smelting of composite pellets in liquid metal bath, including auxiliary studies as back-up investigations with emphasis on kinetics.

4.1 Characterization and Preparations of Raw Materials

In any experimental work, it is extremely important to characterize the input materials as they provide necessary information required for assessment of the properties of the products. These include evaluation of physical, chemical, mechanical, metallurgical and other characteristics of the materials. The sources of raw materials were:

Iron ore : The iron ore was obtained from Tata Steel, Jamshedpur, Jharkhand.
(Source: Noamundi mines, Jharkhand)

Coal : i) Jharia mines, Dhanbad, Jharkhand.
ii) Bhilai Steel Plant, Bhilai, Madhya Pradesh.

Binders : i) Lime : Procured from local market (laboratory reagent grade).
ii) Dextrose : Procured from local market (laboratory reagent grade).
iii) Molasses : Procured from local foundry, Vadodara.
iv) Sodium polyacrylate (SPA): Available at department laboratory.

Charging material : Cast iron (procured from local market).

4.1.1 Size analysis

First of all iron ore lumps were broken into small pieces in jaw and roll crushers. These small pieces were fed into the ball mill. Sufficient number of balls of different sizes, small and large, were put into the ball mill. The milling time was 4 to 5 hours. The impact of balls on the material produced the iron ore powder. The ore powder was

collected in a tray. Similar procedure was followed for coal powder preparation. The milling time was 3 hours. Thorough mixing of each raw material was done before and after size analysis. A porcelain jar was used for mixing. About 1 kg raw material along with eight ceramic balls (20 mm diameter) was kept in the jar, which was then allowed to rotate at 50 rpm for 1 hour.

Size analyses of raw materials were carried out in sieve shaker for 15 minutes. In each case, 200 g sample was taken. Results for iron ore and coal are presented in Table 4.1 and 4.2 respectively.

4.1.2 Chemical analysis of raw materials

(a) Iron ore: Chemical analyses of iron ore were carried out using the following methods:

i) **X-ray Fluorescence (XRF) Spectroscopy:** Chemical analysis of iron ore was carried out by Energy Dispersive X-ray Fluorescence (XRF) Spectrometer (Model: EDXRF-800, Make: Shimazdu, Japan) available at Metallurgical and Materials Engineering Department, M. S. University of Baroda, Vadodara. Measurement conditions were; Sample: powder form, Atmosphere: vacuum, Collimator: 10 mm, Spin: off. The result is reported in Table 4.3.

ii) **Wet analysis:** Potassium dichromate method (volumetric) was used to determine the total iron (Fe_{tot}) content in the iron oxide (Fe_2O_3). Standard procedure, available in the book [166], was followed. Four samples were analyzed and the result is presented in Table 4.3. Similar types of results have also been reported in literature [167, 168] as shown in Table 4.4. That result is nearly matching to ours one.

(b) Coal: The proximate analyses of coals were done according to the standard method. The results (average of three) have been reported in Table 4.5. Coal ash analysis was also done using XRF Spectrometer and results are presented in Table 4.6.

(c) Lime: The quality of lime and the size of the lime particles are of great concern as the lime is used alone or in combination with other binders as binding agent. Small size particles possess large surface area and therefore, larger contact area with iron ore particles. Purity of lime improves the binding strength, makes the slag more fluid and

reduces the slag volume. Analysis of lime was done using XRF Spectrometer and result is reported in Table 4.7.

Table 4.1: Size analysis of iron ore

Mesh Size (ASTM)	Size (micron)	Weight Retained (g)	Weight pct Retained	Cumulative pct Retained	Cumulative pct Passing
+100	+150	39.00	19.50	19.50	80.50
-100 +140	85	115.00	57.60	77.10	22.90
-140 +200	65	42.70	21.40	98.50	1.50
-200 +270	53	2.00	1.00	99.50	0.50
-270 +325	45	1.00	0.50	100.00	0.00
-325 (Pan)	-----	Nil	Nil	-----	-----

Table 4.2: Size analysis of coal

Mesh Size (ASTM)	Size (micron)	Weight Retained (g)	Weight pct Retained	Cumulative pct Retained	Cumulative pct Passing
Coal from Jharia mines					
+100	150	5.00	2.50	2.50	97.50
-100 +140	85	89.20	44.60	47.10	52.90
-140 +200	65	93.70	46.85	93.95	6.05
-200 +270	53	11.10	5.55	99.50	0.50
-270 +325	45	1.00	0.50	100.00	0.00
-325 (Pan)	-----	Nil	Nil	-----	-----
Coal from Bhilai Steel Plant					
+100	150	6.50	3.25	3.25	96.75
-100 +140	85	95.10	47.55	50.80	49.20
-140 +200	65	91.80	45.90	96.70	3.30
-200 +270	53	6.10	3.05	99.75	0.25
-270 +325	45	0.50	0.25	100.00	0.00
-325 (Pan)	-----	Nil	Nil	-----	-----

Table 4.3: Analysis of iron ore

Method	Total Fe (pct)	Fe_2O_3 (pct)	SiO_2 (pct)	Al_2O_3 (pct)	P_2O_5 (pct)	Other Oxides (pct)
XRF	67.40 (calculated)	96.28	1.09	1.41	0.16	balance
Wet (volumetric)	66.40	94.86 (calculated)	-----	-----	-----	-----
Average	66.90	95.57	1.09	1.41	0.16	balance

Table 4.4: Analysis of Noamundi iron ore

Total Fe (pct)	SiO_2 (pct)	Al_2O_3 (pct)	Phosphorous (pct)	Other Oxides (pct)	Ref.
66.90	0.93	1.56	0.059	balance	[167]
66 - 69	0.40 – 1.00	0.45 – 1.95	0.024 – 0.10	balance	[168]

Table 4.5: Proximate analyses of coals

Source of Coal	Moisture (pct)	Volatile Matters (pct)	Ash (pct)	Fixed Carbon (pct)
Jharia mines	0.35	15.65	35.65	48.35
Bhilai Steel Plant	1.33	27.00	14.67	57.00

Table 4.6: Analyses of coal ash

Source of Coal	SiO_2	Al_2O_3	Fe_2O_3	SO_3	CaO	MnO
Jharia mines	55.18	24.57	17.19	2.18	0.73	0.15
Bhilai Steel Plant	45.52	21.96	18.94	4.11	9.33	0.14

Table 4.7: Analysis of lime

CaO (pct)	ZrO_2 (pct)	SrO (pct)
99.85	0.01	0.14

4.1.3 Microstructural observation of raw materials

The Scanning Electron Microscopic (SEM) photomicrographs of iron ore, coal and lime powders are shown in Figure 4.1(a-d). Figure 4.1(a) shows the SEM photomicrographs of iron ore powder sample depicting the presence of mostly spheroidal shaped particles. Some particles are irregular in shape. Figure 4.1(b) shows the SEM photomicrographs of coal powder sample from Jharia mines depicting the presence of mostly irregular shaped particles. Some particles are nearly spherical in shape. Figure 4.1(c) shows the SEM photomicrographs of coal powder sample from Bhilai Steel Plant depicting the presence of mostly irregular shaped particles. Some particles appear to have flaky morphology. A wide variation in particle size is observed. Figure 4.1(d) shows the SEM photomicrographs of lime powder sample depicting the presence of both irregular and spheroidal shaped particles. Variation in particle size is observed minimum.

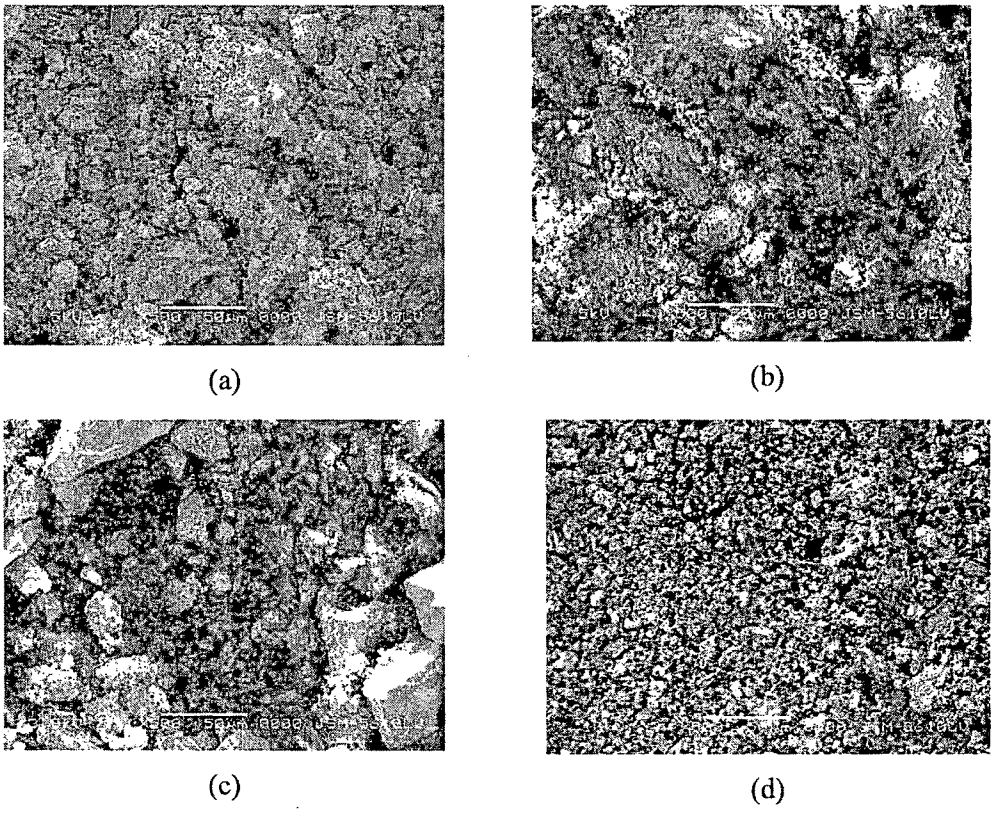

(a) (b)

(c) (d)

Fig. 4.1: SEM photomicrographs of powder samples at 500X (a) iron ore, (b) coal from Jharia mines, (c) coal from Bhilai Steel Plant, and (d) lime.

4.2 Briquette / Pellet Preparation

4.2.1 Briquette preparation

To select the proper binder, initially briquettes of iron ore-coal composite were prepared. Cylindrical shaped briquettes were prepared using a die and punch assembly by giving single impact to the moist powder mixture. The impact was standardized by proper design of assembly. Diameter and height of the briquettes varied from 9.70 to 9.75 mm and 13 to 14 mm respectively. The weight of the briquettes varied between 2.00 to 2.20 g. The green briquettes so formed were exposed to CO_2 gas for 4, 6 and 8 minutes which favoured the formation of carbonate bonds between the particles. These briquettes were dried in open atmosphere for 24 hours followed by oven drying at a temperature of 393 K for 3 hours.

4.2.2 Pellet preparation

Figure 4.2 shows the flow diagram for composite pellet making. Iron ore-coal composite pellets were prepared using slaked lime and dextrose as binder. Binder was selected on the basis of briquettes formation and strength of briquettes. Mixing of raw materials was done in a porcelain jar rotated at 50 rpm for one hour in a pebble mill. Pellets were prepared in batches using a disc pelletizer (400 mm diameter) rotating at 17 rpm. The mix (iron ore fines, coal fines, and binders) was fed into the disc manually and water was added in the form of spray. The moisture was in the range of 8 to 10 pct by weight of the mix. The angle of pelletizer was 40^{O}. The green pellets of nearly 12 to 22 mm size so formed were exposed to CO_2 gas for 6 minutes. These pellets were dried in open atmosphere for 24 hours followed by oven drying at a temperature of 393 K for 3 hours. These pellets get hardened in cold bonding process due to physico-chemical changes of the binder in ambient condition.

For experimental work, composite pellets were prepared using coals from two different sources having four different Fe_{tot}/C_{fix} ratios. The details are presented in the Table 4.8 which shows composition of the iron ore-coal composite pellets.

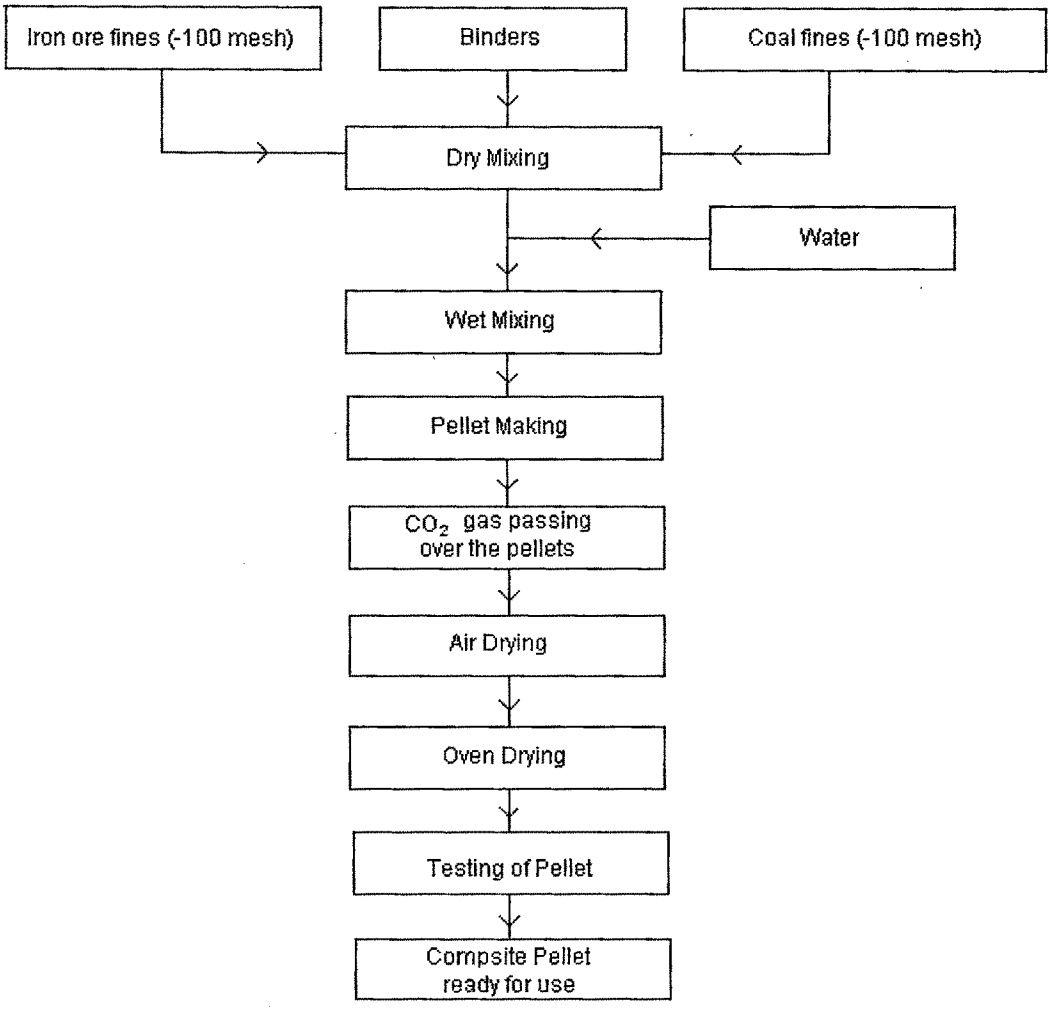

Fig. 4.2: Flow diagram for composite pellet making.

Table 4.8: Composition of iron ore-coal composite pellets

Pellet Code*	Fe_{tot}/C_{fix} Ratio	Iron Ore (pct)	Coal (pct)	Binder (pct)
ACP-1	2.50	58.70	32.49	8.81
ACP-2	3.11	62.70	27.89	9.41
ACP-3	3.50	64.71	25.58	9.71
ACP-4	4.00	66.85	23.12	10.03
BCP-1	2.50	61.75	28.99	9.26
BCP-2	3.11	65.47	24.71	9.82
BCP-3	3.50	67.32	22.58	10.10
BCP-4	4.00	69.28	20.33	10.39

* ACP refers to the composite pellet made with coal from Jharia mines, Dhanbad and
* BCP refers to the composite pellet made with coal from Bhilai Steel Plant, Bhilai.

4.2.3 Microstructural observation of dry composite pellets

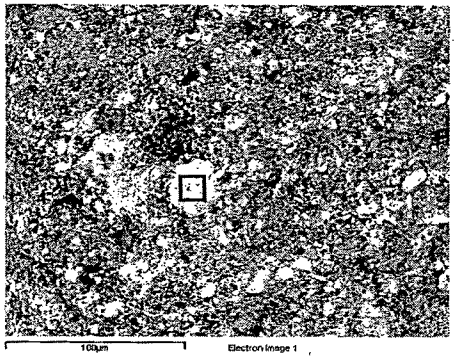

(a): coal from Jharia mines

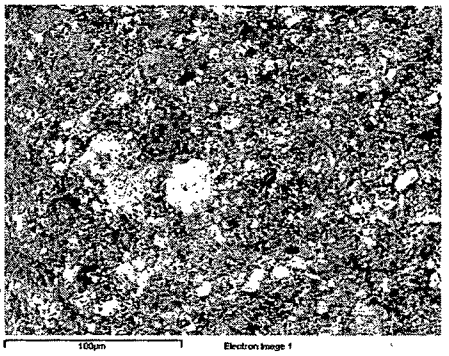

(b): coal from Jharia mines

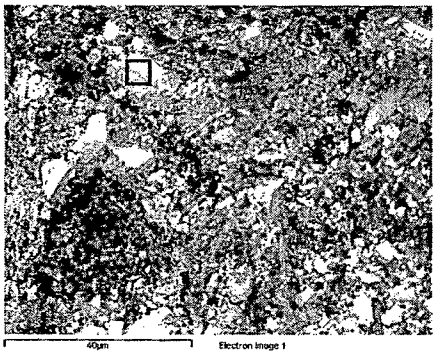

(c): coal from Bhilai Steel Plant

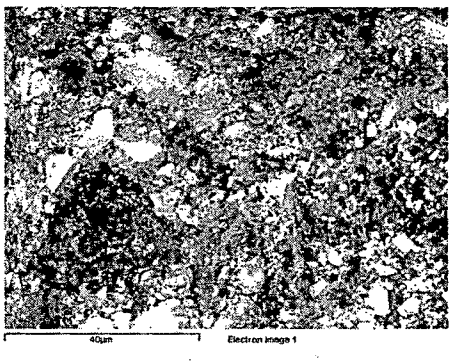

(d): coal from Bhilai Steel Plant

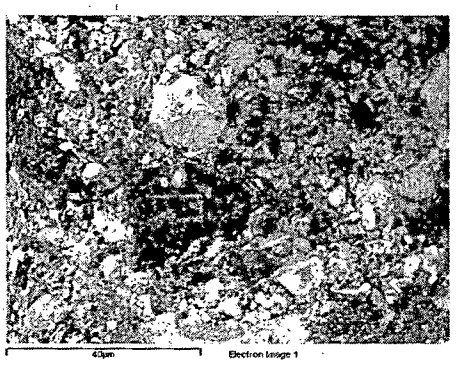

(e): coal from Bhilai Steel Plant

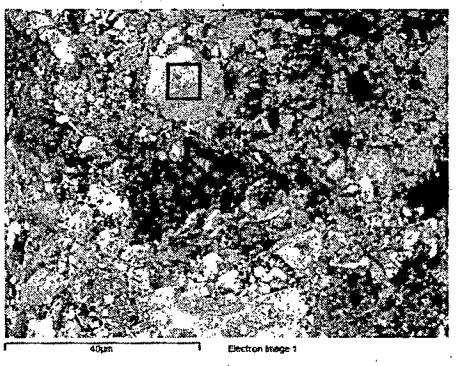

(f): coal from Bhilai Steel Plant

Fig. 4.3: SEM photomicrographs of fractured surface of oven dried iron ore-coal composite pellets (a and b) ACP2 pellet Fe_{tot}/C_{fix} ratio 3.11, (c and d) BCP2 pellet Fe_{tot}/C_{fix} ratio 3.11, and (e and f) BCP1 pellet Fe_{tot}/C_{fix} ratio 2.50.

Figure 4.3 shows the Scanning Electron Microscopic (SEM) photomicrographs of fractured surface (cross section) of oven dried iron ore-coal composite pellets. The morphology of pellets evinces the distribution of iron ore, coal and lime particles reasonably uniform. The Energy Dispersive Analytical X-ray (EDAX) analysis of square marked region in SEM photomicrographs revealed that the bright and grey phases are iron oxide rich and carbon rich regions respectively as shown in Table 4.9. Fine size particles with bright appearance represent lime.

Table 4.9: EDAX analysis of oven dried iron ore-coal composite pellets

Composite Pellet/ Sample Reference	Chemical Composition (wt pct)					
	Fe	O	C	Al	Si	Ca
ACP2, Fig 4.2(a)	54.64	29.66	12.82	0.88	0.67	1.33
ACP2, Fig 4.2(b)	7.53	21.16	68.51	0.65	1.18	0.97
BCP2, Fig 4.2©	65.84	26.18	5.52	0.54	0.72	1.20
BCP2, Fig 4.2(d)	5.70	31.80	58.95	0.44	0.99	2.12
BCP1, Fig 4.2(e)	2.95	24.96	68.35	1.61	1.34	0.79
BCP1, Fig 4.2(f)	61.11	25.17	10.94	0.11	0.08	2.59

4.3 Testing of Briquettes / Pellets

The properties of briquettes / pellets of interest are those properties which have bearing on its performance during handling and transportation until it is charged in the furnace, and subsequently on its behaviour inside the furnace. The success of the cold bonding process depends heavily on attaining sufficient strength of the composite pellets. Some of the room temperature physical and mechanical properties have been tested and results are reported in this section.

4.3.1 Density of pellet

Both apparent and true densities of pellets were measured based on the Archimedes' principle.

(a) Apparent density of pellet: Moisture free pellet was taken and a thin layer of silicon grease was applied on its surface to make the pellet impervious to water. Weight of the

pellet in air (W_{1a} kg) was taken using physical balance. The pellet was tied with a thin wire and arrangement was made to take the weight of the pellet submerged in water (W_{2a} kg). Apparent weight loss of pellet [(W_{1a}-W_{2a}) kg] was found and the apparent density of pellet was calculated as follows.

$$\rho_a = \left(\frac{\text{Weight of the pellet in air}}{\text{Weight of water displaced by the completely submerged pellet}} \right)$$

$$= \left(\frac{\text{Weight of the pellet in air}}{\text{Apparent weight loss of pellet in water}} \right)$$

$$= \left(\frac{W_{1a}}{W_{1a} - W_{2a}} \right) kg.m^{-3} \quad \text{.....(4.1)}$$

Where, ρ_a = Apparent density of pellet, $kg.m^{-3}$

W_{1a} = Weight of the pellet in air, kg

W_{2a} = Weight of the pellet in water, kg

(b) True density of pellet: Similar procedure was used as apparent density determination. The only difference was that the dry pellet was put in water for an hour or till the complete air entrapped in the pores of pellet got released. Here, no greasing of pellet was done. Calculation for true density determination was done as follows.

$$\rho_t = \left(\frac{\text{Weight of the water soaked pellet in air}}{\text{Weight of water displaced by the completely submerged pellet}} \right)$$

$$= \left(\frac{\text{Weight of the water soaked pellet in air}}{\text{Weight loss of water soaked pellet in water}} \right)$$

$$= \left(\frac{W_{1t}}{W_{1t} - W_{2t}} \right) kg.m^{-3} \quad \text{.....(4.2)}$$

Where, ρ_t = True density of pellet, $kg.m^{-3}$

W_{1t} = Weight of the water soaked pellet in air, kg

W_{2t} = Weight of the water soaked pellet in water, kg

4.3.2 Porosity of pellet

Porosity is expressed as the volume of pores as a percentage of the total volume of the material. It is usually measured by simple method based on Archimedes' principle. It is a

very important property from the reduction point of view. The reducibility of an ore or pellet increases as the porosity is raised. Porosity is vital in green pellets, which are intended for subsequent heat hardening or reduction. Basically, it is governed by the particle size of the feed stock but may be affected by balling [24]. For green pellets, the compressive strength depends on the pellet size, composition, porosity and the saturation degree of the pores [169]. Kinetically, reduction of oxides in iron ore-coal composite pellet is significantly by carbon. The carbothermic reduction of iron oxides takes place through gaseous intermediate. Diffusion of reducing gases into the lump, pellet or sinter depends on the porosity. Reduction reaction in composite pellets is controlled by gasification reaction which involves both chemical reaction and pore diffusion. The reducing gases diffuse through the micropores or cracks of the product layer to reach reaction interface.

The porosity of the pellet was calculated as follows.

$$\text{Porosity (pct)} = \left(\frac{\text{True density} - \text{Apparent density}}{\text{True density}} \right) \times 100 \quad \text{.....(4.3)}$$

Results of pellet densities and porosity have been reported in Table 4.10.

Table 4.10: Physical properties (density and porosity) of pellets

Composite Pellet*	Fe_{tot}/C_{fix} Ratio	Apparent Density ($kg.m^{-3}$)	True Density ($kg.m^{-3}$)	Porosity (pct)
ACP-1	2.50	2.158×10^3	2.872×10^3	24.86
ACP-2	3.11	2.257×10^3	2.918×10^3	22.65
ACP-3	3.50	2.421×10^3	2.931×10^3	17.40
ACP-4	4.00	2.546×10^3	3.020×10^3	15.70
BCP-1	2.50	2.077×10^3	2.701×10^3	23.10
BCP-2	3.11	2.161×10^3	2.649×10^3	18.42
BCP-3	3.50	2.346×10^3	2.805×10^3	16.36
BCP-4	4.00	2.465×10^3	2.851×10^3	13.54

* ACP refers to the composite pellet made with coal from Jharia mines, Dhanbad and
* BCP refers to the composite pellet made with coal from Bhilai Steel Plant, Bhilai.

It was observed that for both ACP and BCP pellets the values of porosity decreased with increasing Fe_{tot}/C_{fix} ratio as shown in Figure 4.4. This is attributed to the increasing amount of iron ore vis-à-vis decreasing amount of coal in pellets with increasing Fe_{tot}/C_{fix} ratio. Further, the porosity of BCP pellets were found lower than ACP pellets for corresponding Fe_{tot}/C_{fix} ratio which may be attributed to the relatively higher amount of iron ore vis-a-vis lower amount of coal in corresponding Fe_{tot}/C_{fix} ratio pellets (as shown in Table 4.8) as well as low ash content in Bhilai coal.

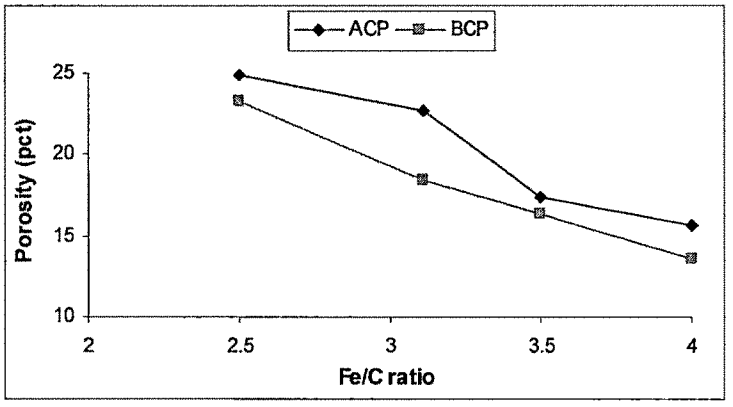

Fig. 4.4: Porosity of iron ore-coal composite pellets.

4.3.3 Strength properties of briquette / pellet

The briquettes / pellets have been subjected to the following tests.

i) Drop test: In the drop test, the briquettes or pellets were dropped repeatedly from a height of 0.45 m on a 10 mm thick steel plate until they break. The number of drops, before breaking of the pellet, was counted and noted down. The final value was taken as the average of four such test values.

ii) Compression test: This test was performed by applying uniaxial compressive load at a constant rate and compressive strength was taken as the force required to break the briquette / pellet. Each briquette / pellet was squeezed between two plates under increasingly applied load. The value of the load at which the briquette developed crack was recorded as strength. The final value was calculated as the arithmetic mean of four such test values.

The compressive strengths of the briquettes were measured on tensometer (Make: Mikrotech, Pune). The testing results for briquettes are presented in Table 4.11. The pellets were tested on compressive strength testing instrument (Digital Force Gauge, Model: HEM-FG-250 kg, Make/Supplier: HEMETEK Techno Instruments Pvt. Ltd., Vadodara) at R&D Centre of Electrotherm India Ltd., Ahmedabad. This instrument is precise and highly reliable. The results were found reproducible and have been presented in Table 4.12.

iii) Shatter test: The known amounts of briquettes / pellets were dropped from a standard height of 2 m on a 10 mm thick steel plate for 4 times [170]. The broken sample pieces were put on a 100 mesh sieve. The amount of the material, expressed as percentage of the original weight, passed through the sieve was indicated as the shatter index.

$$\text{Shatter index} = \left(\frac{weight\ of\ -100\ mesh\ size\ particles}{Total\ weight\ of\ sample\ taken} \right) \times 100 \quad \text{.....(4.4)}$$

4.3.3.1 Testing results for briquettes

The compressive strength values as shown in Table 4.11 represent the average of four measured values of briquettes' strength. The values varied mostly by ± 15 pct from the average value of sample. It was observed that the maximum strength was obtained with 6 minutes of CO_2 gas exposure to briquettes than that of 4 and 8 minutes gas exposure. This may be attributed to the optimum CO_2 gas exposure required for carbonate bond formation. Over-gassing or under-gassing may cause the bonding to become weak after drying of briquettes. Another observation was that the highest strength (357 N/briquette) was obtained for briquettes prepared by slaked lime plus dextrose as binder. The organic binder tends to form polymer bridges at the point of contact between the particles to ensure good dry strength of pellets. Therefore, slaked lime and dextrose were selected as binder for composite pellet preparation.

Similar result was obtained for drop strength of briquettes. Here also, the maximum strength was obtained with 6 minutes of CO_2 gas exposure to pellets than that of 4 and 8 minutes gas exposure. The highest drop strength was obtained for briquettes prepared by slaked lime plus dextrose as binder and 6 minutes of CO_2 gas exposure.

In all cases, shatter index values were observed lower for 6 minutes CO_2 gas exposure and lowest for slaked lime plus dextrose.

Table 4.11: Dry strength of composites briquettes

- All pct wt w. r. t. weight of iron ore
- Coal: Jharia mines
- $Fe_{total}/C_{fix} = 3.11$ (stoichiometric ratio)
- Treatment: First air drying (24 hrs); then dried in oven (at 393 K for 3 hrs)

Binder	Binder (wt pct)	CO_2 Gas Passed for (mins)	Compressive Strength* (N/Briquette)	Shatter Index (pct)	Drop Strength* (numbers)
Lime (CaO)	10	4	120	4.43	32
		6	137	3.86	46
		8	113	5.29	27
$Ca(OH)_2$	10	4	128	3.69	40
		6	142	3.43	56
		8	118	4.07	34
Slaked lime	10	4	134	2.45	48
		6	162	1.89	65
		8	127	2.71	40
CaO + Dextrose	10 + 5	4	232	1.04	52
		6	250	0.86	68
		8	197	1.32	47
Slaked lime + Dextrose	10 + 5	4	292	0.52	65
		6	357	0.44	84
		8	271	0.64	58
CaO + Slaked lime + Dextrose	5 + 5 + 5	4	241	0.90	55
		6	263	0.74	70
		8	226	1.26	48
$Ca(OH)_2$ + Molasses	10 + 5	4	255	0.81	64
		6	280	0.53	75
		8	231	0.94	54
Slaked lime + Molasses	10 + 5	4	276	0.67	65
		6	299	0.48	82
		8	255	0.76	45
Sodium Polyacrylate (SPA)	10	4	235	1.54	46
		6	240	1.37	53
		8	216	1.80	38
SPA + Slaked lime	5 +5	4	123	1.87	39
		6	142	1.59	44
		8	108	2.52	36

* Average of four measurements.

4.3.3.2 Testing results for pellets

The compressive strength values as shown in Table 4.12 represent the average of four measured values of pellets' strength. The values varied mostly by ± 15 pct from the average value of sample. For ACP pellets, the maximum and minimum strengths of 330 and 212 N/pellet were obtained for Fe_{tot}/C_{fix} ratio of 4.0 and 2.5 respectively. Similarly, for BCP pellets, the maximum and minimum strengths of 362 and 240 N/pellet were obtained for Fe_{tot}/C_{fix} ratio of 4.0 and 2.5 respectively.

Table 4.12: Dry strength of composite pellets

- ACP : Pellets prepared with coal from Jharia mines
- BCP: Pellets prepared with coal from Bhilai Steel Plant
- Binders used: Slacked lime and Dextrose
- CO_2 gas was passed for 6 minutes
- Treatment: First air drying (24 hrs); then dried in oven (at 393 K for 3 hrs)
- Average size pf the pellet: 16 - 19 mm

Pellet Code*	Fe_{tot}/C_{fix} Ratio	Binder (pct)	Porosity of Pellet (pct)	Compressive Strength# (N/Pellet)	Shatter Index (pct)	Drop Strength# (numbers)
ACP-1	2.50	8.81	24.85	212	1.133	43
ACP-2	3.11	9.41	22.65	244	0.923	50
ACP-3	3.50	9.71	17.42	273	0.609	58
ACP-4	4.00	10.03	15.70	330	0.336	74
BCP-1	2.50	9.26	23.27	240	1.167	47
BCP-2	3.11	9.82	18.42	278	0.910	56
BCP-3	3.50	10.10	16.40	310	0.585	68
BCP-4	4.00	10.39	13.54	362	0.245	82

* ACP refers to the composite pellet made with coal from Jharia mines, Dhanbad and

* BCP refers to the composite pellet made with coal from Bhilai Steel Plant, Bhilai.

Average of four measurements.

It was observed that the average compressive strength of both ACP and BCP pellets increased with increasing Fe_{tot}/C_{fix} ratio as shown in Figure 4.5. This may be attributed to the higher ratio of iron to carbon as well as more amount of binder in pellets. Further, the compressive strength of BCP pellets were found higher than ACP pellets for corresponding Fe_{tot}/C_{fix} ratio which may be attributed to the relatively higher amount of binder as well as low porosity.

Similar trend was observed for drop strength of pellets as shown in Figure 4.6. The shatter index values were observed decreasing with increasing Fe_{tot}/C_{fix} ratio in both ACP and BCP pellets as shown in Figure 4.7.

The strengths of the oven dried pellets as a function of porosity are shown in Figures 4.8 and 4.9. It was observed that with increase in porosity both the compressive and drop strengths decreased. Similar result was reported in literature [24]. Mantovani et al [169] also observed similar result and concluded that the compressive strength of green pellets depends on the pellet size, its composition, porosity and the saturation degree of the pores.

4.4 Flow Rate of Argon Gas

The flow rate measurement of argon gas was carried out using a simple standard graduated burette with soap solution. It was necessary to carry out this experiment to get the correct flow rate of the gas. A graph was plotted between flow rate *vs* liquid height difference in tube as shown in Figure 4.10.

4.5 Induction Furnace

4.5.1 Principle: Induction melting furnace is basically a transformer in which the primary side is the furnace coil through which the current flows; and the charge, being melted and/or superheated, acting as short circuited secondary. Due to the electrical current passing through the power coil eddy current is induced in the charge, which generates heat within the charge.

There is no need of heat transfer to the charge because heat is generated within the charge itself. Therefore, there is no limit of the maximum attainable temperature except that

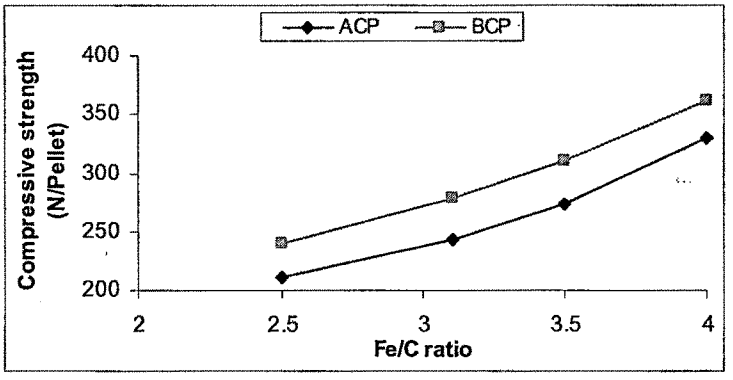

Fig. 4.5: Compressive strength *vs* temperature plot for pellets.

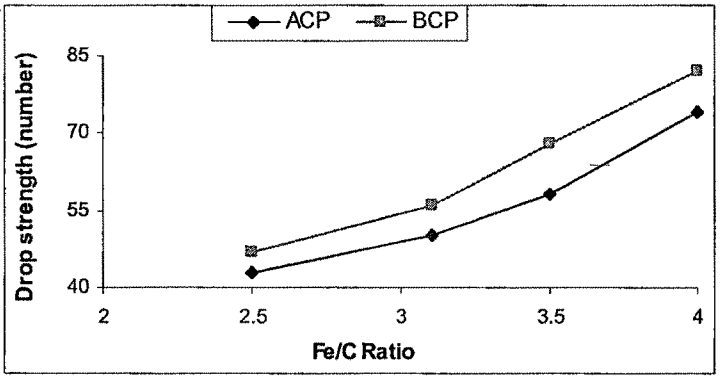

Fig. 4.6: Drop strength *vs* temperature plot for pellets.

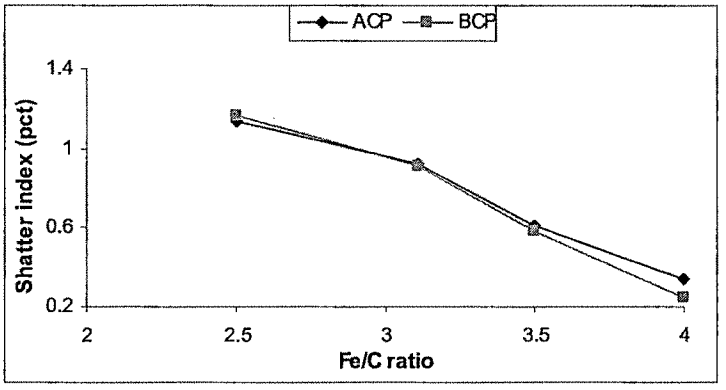

Fig. 4.7: Shatter index *vs* Fe/C ratio plot for pellets.

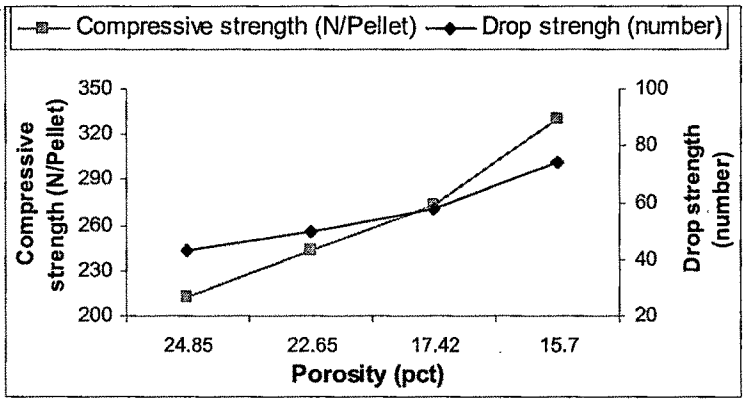

Fig. 4.8: Strength *vs* porosity plot for ACP pellets.

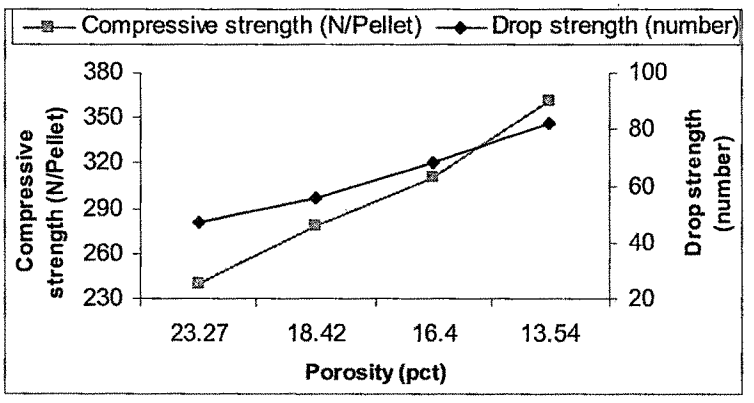

Fig. 4.9: Strength *vs* porosity plot for BCP pellets.

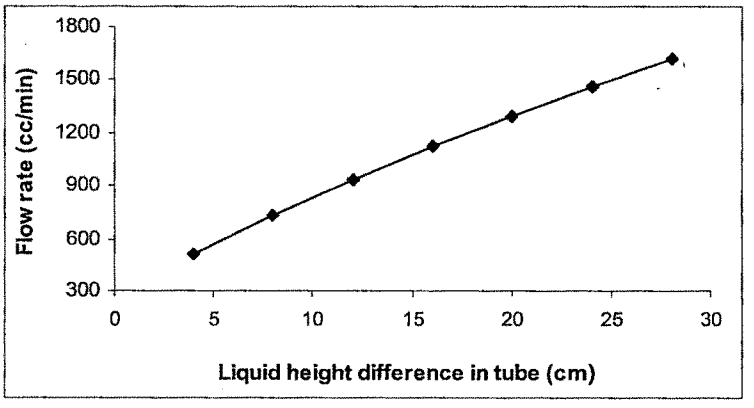

Fig. 4.10: Flow rate of argon gas.

imposed by the material of the rammed crucible and the metallurgical behaviour of metal-slag-lining atmosphere interaction. It is, therefore, very likely to excessively superheat the melt, if the furnace operators are not vigilant enough. From the standpoint of thermal engineering, an induction furnace is a nearly perfect system, since the heat is generated in the place where it is to be consumed [171].

4.5.2 Theory of induction heating [172]

The coreless induction furnace consists of a refractory container, capable of holding the molten bath, which is surrounded by water-cooled helical coil connected to a source of alternating current. Induction heating is the heating of an electrically conducting object immersed in a varying magnetic field. An alternating electromagnetic field induces eddy currents in the metal thereby electrical energy gets converted to heat. The quantity of heat evolved depends on the resistivity of the charge. The object being heated need not be a magnetic material to heat efficiently. All that is required is that it should have reasonably good electrical conductivity.

In coreless induction furnaces, lines of magnetic force close through the air, which offers a large resistance to their passage and thus significantly reduces the useful magnetic fluxes. The electromagnetic force (emf) of induction is as follows:

$$\text{emf} = (4.44) \times \phi_{max} \times f \times n \times 10^{-8} \text{ V} \qquad \text{.....(4.5)}$$

Where, n = number of inductor turns,

f = alternating current frequency, and

ϕ_{max} = magnetic flux density

If φ_{max} drops, the required emf of induction can be retained by increasing current frequencies. In that case the magnetic flux will change frequently. The emf induced in the metallic charge forms whirl currents in the plane of the winding turns. The density of induced currents attains its maximum at the surface of the charge and lowers towards the middle. This phenomenon of displacement of electric current to the surface has been termed *skin effect.*

As is known, AC current distributes unevenly over the cross-section of a conductor, which is linked with the fact that the inner layers of the conductor are enveloped by a

greater magnetic flux, have a higher inductance and therefore, higher impedance. The depth of the surface layer of a metal where the density of induced current is large called penetration depth. The heat required to melt the charge is developed mainly in that layer. The penetration depth may be found by the formula:

$$D_p = 5.03 \times 10^3 \times \sqrt{\frac{\rho_r}{\mu f}} \qquad \text{.....(4.6)}$$

Where, D_p = depth of penetration

ρ_r = Resistivity of the charge, Ohm-cm

μ = magnetic permeability

f = frequency, Hz

Large surface require lower frequency than smaller ones. The energy that is transformed into heat in the charge is as follows:

$$W = I^2 \times n^2 \times 2\pi^2 \times \frac{d}{h} \times \sqrt{\rho_r \mu f \times 10^{-9}} \qquad \text{.....(4.7)}$$

Where, I = current in the conductor, A

n = number of inductor turns

d = mean diameter of crucible, cm

h = depth of metal in the crucible, cm

The product (I x n) is called ampere-turns. The energy that is transformed into heat in the charge is directly proportional to the square of the ampere-turns and to the square root of Resistivity and frequency.

4.5.3 Advantages of induction furnace [173]

Melting in induction furnace offers the following advantages:

i) Induction furnaces have high flexibility in which even a small quantity of metal of any composition can be melted. The furnace can be started with the cold charge and no molten metal-hill is required. The melting process is also quite simple.

ii) The induction furnaces have an extremely high rate of melting. The melting time is generally about one hour due to higher power to charge ratio.

iii) The control of temperature is very easily and quickly obtained within a wide range.

iv) Highly alloyed steels can be melted without appreciable loss of alloying elements. The actual metallic yield of liquid steel from scrap is also exceptionally good.

v) Clean atmosphere in the furnace during melting leads to efficient control of composition.

vi) The electromagnetic forces acting on the melt cause an intensive bath movement that gives efficient stirring action and homogenize the melt.

vii) High quality metal and alloys, free of hydrogen and nitrogen, can be produced by this method.

viii) Operating costs are lower because of low refractory consumption, low power consumption, absence of electrodes, better heat utilization, and shorter melting time.

ix) Requires less floor space and relatively free from pollution.

4.5.4 Lining of induction furnace

First of all, the damaged crucible and the broken lining materials were removed and the alumina paste was applied around the helical copper coil. This alumina paste protects the induction coil. The paste was allowed to dry for a day. Thereafter, the furnace bottom was properly leveled with alumina ramming mass. 2 mm thick glass wool fiber sheet was put around the dried paste. The steel former was placed at the centre of the melting pot. The gap between glass wool and steel former was filled by dry alumina ramming mass. Ramming was done manually. The top of the rammed portion around the steel former was capped with alumina paste and a suitable vane was made for easy pouring of the melt. This was allowed to air dry for two days. After that the furnace was filled with cast iron scrap as charge material and furnace was put on power at zero watt for 2 hours for complete drying and preheating of the lining. Now, the lining is ready for the melt. For few heats the lining was done with ramming mass of magnesite.

4.5.5 Mould preparation

Sand mould was prepared before the heat. Green sand and bentonite were mixed thoroughly in muller with approximately 2 pct bentonite and 9 pct water to prepare the moulding sand. Cope and drag portion of the mould box was first filled with the moulding sand and then ramming was done. Vertical mould cavities were made by

piercing cylindrical wooden rods in the rammed moulding sand. Venting was done to facilitate the easy escape of gases generated during casting.

4.6 Experiment

4.6.1 Pyrolysis of coal

Coal pyrolysis is discussed in detail in Section 2.1.2.2. Since coal was used as reductant for iron oxides, so during heating of composite pellets, devolatilization of coal also occurred simultaneously. To know the rate of devolatilization, separate studies on TG-DTA of coals were carried out. TG-DTA of coals were carried out in SEIKO TG-DTA-32 Simultaneous Thermal Analyzer in platinum crucible (Make: SII, SEIKO Instruments, Japan) in the temperature range of 298 to 1273 K at a heating rate of 15 K/min. Alpha alumina was used as reference material. The atmosphere inside the furnace chamber was maintained inert by flowing argon gas at 300 cc/min. Continuous monitoring of the instrument operation, temperature control, measurements of changes in weight and enthalpy, and storage of data was done by the computer interfaced with the TG-DTA apparatus. TG-DTA plots were obtained by a plotter attached with computer.

4.6.2 Non-isothermal studies of iron ore-coal composite pellets

Non-isothermal reduction studies of iron ore-coal composite pellets were also carried out in SEIKO TG-DTA-32 Simultaneous Thermal Analyzer in platinum crucible to investigate the reduction behaviour of composite pellets. Alpha alumina was used as reference material. Around 8.5 mg of powder sample was used in each run. The reduction temperature range was set from ambient to 1473 K at heating rate of 10 K/min. The atmosphere inside the furnace chamber was maintained inert by flowing argon gas at 300 cc/min. Continuous monitoring of the instrument operation, temperature control, measurement of change in weight and enthalpy, and storage of data was done by the computer interfaced with the TG-DTA apparatus. After the run was over, argon gas flow continued till the sample temperature dropped to 773 K. Few experiments were conducted with heating rate of 15 K/min. TG-DTA plots were obtained by using a plotter attached with computer. Variables for non-isothermal reduction studies of composite pellets are listed in Table 4.13.

Table 4.13: Variables for non-isothermal reduction of composite pellets

Sl. No.	Variable	Number	Remarks
1.	Iron ore	1	Noamundi mines
2.	Coal	2	Jharia mines, and Bhilai Steel Plant
3.	Fe_{tot} / C_{fix} ration in pellet	4	2.50, 3.11, 3.50 and 4.00
4.	Maximum temperature	1	1473 K
5.	Heating rate	1	10 K/min

4.6.3 Kinetics of smelting of composite pellets in an induction furnace

Smelting reduction of iron ore-coal composite pellets was carried out in a laboratory induction furnace (Make: Inductotherm Corporation, New Jersey, USA) having 15 kW power rating and 6 kg melt capacity as shown in Photo 4.1. The unit operates on 460 V, three-phase, 50 Hz, 20 kVA power source with an output of 9600 Hz. It is a variable induction power (VIP) furnace having two types of water cooling system:

i) a closed loop internal system which circulates demineralized water and includes the heat exchanger, and

ii) an external water system which provides water to cool shell and heat exchanger of the internal system and also the furnace coil.

The experiments were designed to investigate the reduction kinetics and dissolution behaviour of composite pellets in liquid metal bath. Before switching on the furnace, the demineralized water circulation through heating coil and induction panel was set on. The furnace crucible was filled with cast iron scrap and furnace was switched on with initial power supply of 4-5 kWh and gradually raised to 10 kWh. Within half an hour the cast iron scrap melted and liquid metal bath was ready for the kinetic studies. High purity argon gas (containing 2 ppm oxygen only) at a flow rate of 1500 cc/min was passed on to avoid the oxidation of the liquid metal bath surface. For kinetics studies, the pellets of known weight were tied with tungsten wire. These pellets were initially preheated for 2 minutes and then immersed in liquid metal bath for 10, 20, 30, 40 and 50 seconds. After immersing the pellets for predetermined period of time, the pellets were taken out and quickly transferred to the desiccator to prevent oxidation. The weight loss of each pellet

was measured using electronic balance. Calculations were carried out to find out the fraction of reduction and other kinetic parameters.

Photo 4.1: Smelting reduction set-up (induction furnace with power control panel).

To study the dissolution behaviour of composite pellets in liquid metal bath, a single pellet was thrown in the liquid metal bath and was visually observed that how the pellet dissolves in the metal bath and the time required for complete dissolution was noted. This was repeated several times. Few partially dissolved pellets were collected for scanning electron microscopic examination. Variables for kinetic studies of smelting reduction of composite pellets are listed in Table 4.14.

Table 4.14: Variables for kinetics of smelting of composite pellets

Sl. No.	Variable	Number	Remarks
1.	Iron ore	1	Noamundi mines
2.	Coal	2	Jharia mines, and Bhilai Steel Plant
3.	Fe_{tot}/C_{fix} ratio in pellet	4	2.50, 3.11, 3.50 and 4.00
4.	Time, s	5	10, 20, 30, 40 and 50
5.	Bath temperature, K	1	1723 ± 10
6.	Argon gas flow rate, cc/min	1	1500

4.6.4 Bulk dissolution of composite pellets and iron recovery

The experiments were carried out to observe the bulk dissolution of composite pellets in liquid metal bath and to assess the recovery of iron (in terms of yield). Initially the furnace crucible was filled with cast iron scrap. Before switching on the furnace, the demineralized water circulation through heating coil and induction panel was set on. The furnace was given the initial power of 4-5 kWh and then gradually the power was raised to 10 kWh. Within half an hour the cast iron scrap melted and formed hot-heel. High purity argon gas (containing 2 ppm oxygen only) at a flow rate of 1500 cc/min was passed on to avoid the oxidation of the liquid metal bath surface.

A small amount of liquid metal sample was collected for initial chemical analysis. Composite pellets were charged in small batches in hot-heel. Preheating of pellets took place due to the heat radiation from hot-heel and subsequently reduction and dissolution of pellets occurred in hot-heel. After complete dissolution of pellets and slag-off, the liquid metal bath was allowed to homogenize for some time. The fluidity of metal bath increased with time which led to the homogenization of bath due to convective stirring within liquid metal. The temperature of the liquid metal bath was measured by immersion thermocouple (Pt, Pt-10 pct Rh) and was maintained in the range of 1723 ± 10 K. A precise control over power feeding system to the induction furnace could help in maintaining the temperature within desired range. Slag removal was done by steel rod. Liquid metal was poured in sand mould. The casting was knocked out after solidification and samples were cut for chemical analysis.

Recovery of iron (i.e. yield) was calculated as follows:

$$\text{Iron yield (pct)} = \left(\frac{\text{Total iron in output cast samples}}{\text{Total iron in input materials}} \right) \times 100 \qquad \text{.....(4.8)}$$

4.7 Scanning Electron Microscopy (SEM) and EDAX Analysis

Scanning electron microscopy (SEM) is used primarily for the study of surface topography of solid materials. It permits a depth of field far greater than optical or transmission electron microscopy (TEM). The resolution of the SEM is about 3 nm, approximately two orders of magnitude greater than the optical microscope and one order

of magnitude less than the TEM. Thus, the SEM bridges the gap between the other two techniques [174].

Scanning electron microscopic examinations of the powder samples of iron ore, coal and lime were carried out to observe the size and shape morphology using JEOL SEM (Model: JSM-5610 LV) coupled with Oxford Energy Dispersive Analytical X-ray (EDAX) system. Further, fractured surface of dry composite pellets and reduced pellets was observed under SEM. Few photographs of SEM observations were taken and spectrum of elemental distribution and chemical (elemental) analysis of selected spots were carried out by EDAX system.

4.8 X-ray Diffraction (XRD) Studies

The diffraction of X-ray is of great analytical significance, as it is used to obtain information about the structure, composition, and state of polycrystalline materials. XRD is adaptable to quantitative applications, because the intensities of the diffraction peaks of a given compound in a mixture are proportional to the fraction of the material in the mixture [175]. X-ray diffractometers are basically analogous to an optical grating spectrometer, with the difference that lenses and mirrors are not used with X-rays. Therefore, they appear quite different from their counterparts.

The X-ray diffraction tests of reduced pellets were carried out using Rigaku D. Max III Geigerflex X-ray Diffractometer (Specification: 3 kVA capacity, 20 to 30 kV, 2.5 to 80 μA, Cu/Mo target, Scan angle 3 to 160^0, Scintillating counter) to identify the phases present in reduced pellets.

A few samples were selected for X-ray diffraction studies. Samples were collected after reduction of composite pellets in molten metal bath. By hand grinding, reduced samples were powdered and spread on a glass slide coated with thin film of silicon grease. With the help of another slide, the powder was spread uniformly on the slide. Then the sample was placed in the holding chamber for X-ray diffraction. The CuK_α monochromatic X-ray radiations were utilized to record the XRD spectrum of samples over spectral span of 10 to 90^0. X-rays were generated by imposing 1.0 kV potential difference across the cathode, while maintaining a generator current at 300 mA. The wavelength of X-rays

generated with Cu target was 1.5405 Å. The step size and scan speed were 0.010 and 3 degree/min respectively. Diffraction pattern was recorded and the phase identification was carried out by matching the peaks with powder diffraction patterns given in Powder Diffraction Handbooks (sets 1-30), published by Joint Committee on Powder diffraction Standards, Philadelphia, Pennsylvania, USA.

4.9 Energy Dispersive X-ray Fluorescence (XRF) Spectrometer

X-ray fluorescence (XRF) Spectroscopy is an extremely powerful tool for qualitative and quantitative determination of heavy elements in the presence of each other and in any matrix. It is a relatively simple and, in general, nondestructive method for the analytical determination of elements. It is based on the principle that the energy of the emitted X-rays depends on the atomic number (Z) of the element and their intensity depends on the concentration of the atom in the sample [175]. There are two types of experimental equipment available. One is based on wavelength dispersive XRF and the other is based on energy dispersive XRF. They differ only in the manner the emitted radiation from the sample is dispersed. The wavelength dispersive XRF uses a crystal grating to separate the energies while XRF uses a solid state detector. XRF has the advantage of speed but the disadvantage of poorer sensitivity and resolution [174].

XRF Spectrometer (Model: EDXRF-800, Make: Shimazdu, Japan, Resolution: 155 eV, Rh target with 5 to 500 kV, 8 samples turret, Sample analysis range of elements: C to U) is very useful analytical instruments for analysis of both homogeneous and heterogeneous materials, especially for samples of unknown chemistry. XRF unit includes X-ray generator, vacuum unit, automatic collimator, solid state Li detector, sample turret and microcomputer. It is equipped with a high level fundamental parameter (FP) software for qualitative and quantitative analysis of totally unknown sample. The X-ray tube has Rhodium (Rh) target having 5 to 50 kV voltage and 1 to 1000 μA current range.

It makes use of X-rays to excite an unknown sample surface. The EDXRF-800 can automatically identify all elements in a sample based upon a library of X-ray data, i.e., it also contains matching software providing standardless analysis. The energy level indicates the element involved, and the number of pulses counted at each energy level

over the entire counting time is related to the concentration of the element. Sample can be analyzed either in air or vacuum or helium. For quantitative analysis, either of the two techniques namely fundamental parameter (FP) method or calibration curve (CC) method can be used. The later method is more accurate than the former one. XRF technique is inherently very precise and is attractive for elements which lack reliable wet chemical methods, such as tantalum and rare earths.

4.10 Chemical Analysis Using Optical Emission Spectrometer (OES)

When a substance is correctly excited by an electrical arc or spark, every element present emits light at wavelengths that are specific for that element. The light emitted passes through a narrow vertical slit and is dispersed with a grating or prism. The location and intensity of the spectral lines produced by the samples are compared with the lines produced by suitable standards of known composition. Emission spectrographic technique can be applied to almost every type of sample [174].

The chemical analysis of metal samples of castings produced by smelting of composite pellets was carried out by Optical Emission Spectrometer (OES) at AIA Engineering Ltd., Odhav, Ahmedabad. This is iron based metal analyzer (Optical Emission Spectrometer, Model: 3460, Make: Thermo Applied research Laboratory, Switzerland) capable of analyzing the elements to the fourth digit after decimal. Two samples (one collected before the charging of composite pellets i.e. initial sample and the second after complete dissolution of composite pellets i.e. final sample) were analyzed from each heat.

For precise analysis of carbon and sulphur, the samples were analyzed by LECO carbon-sulphur analyzer (Model: 448, Make: LECO Corporation, USA) at AIA Engineering Ltd., Odhav, Ahmedabad. This equipment is considered to be the most reliable as far as the analysis of carbon and sulphur is concerned. One gram of chips is required for chemical analysis. Two samples from each heat were analyzed.